PHYSICAL REVIEW C VOLUME 13, NUMBER 1 JANUARY 1976

# Decay of $^{36}$K†

Martin J. Fritts*
*Nuclear Physics Laboratory, Department of Physics and Astrophysics, University of Colorado, Boulder, Colorado 80302*
(Received 18 August 1975)

$^{36}$K was produced via the $^{36}$Ar$(p,n)^{36}$K reaction. Measurement of 27 $\beta^+$ delayed $\gamma$ rays associated with the decay of $^{36}$K implied 10 new $\beta^+$ branches to energy levels in $^{36}$Ar. Branching ratios and log$ft$ values are calculated for the $\beta^+$ branches. Restrictions on spin and parity assignments for the $^{36}$Ar levels are given, as well as branching ratios for $\gamma$ transitions from these levels. The half-life of $^{36}$K is determined to be 344±3 msec.

[RADIOACTIVITY $^{36}$K[from $^{36}$Ar$(p,n)$, $E$ = 18 MeV]; measured $E_\gamma$, $I_\gamma$, $\tau_{1/2}$; deduced $\beta^+$ branching ratios, log$ft$'s, $^{36}$Ar levels $l^\pi$; enriched targets.]

## I. INTRODUCTION

This investigation was undertaken to obtain more detailed information on the decay of $^{36}$K. Recent measurements[1] of this decay have produced additional data on the subsequent $\gamma$ decay of populated levels in $^{36}$Ar, implying values for $\beta^+$ branches and log $ft$'s significantly different from those found in earlier work.[2] Yet both experiments agreed that the decay proceeded through $\beta^+$ branches to the 6.61, 4.44, and 1.97 MeV levels. However, the $Q$ value for the decay is 12.8 MeV,[3] and it was possible that other weaker branches might exist which could supplement the available information on spins, parities, and branching ratios obtained through other experiments, particularly $^{35}$Cl$(p,\gamma)$ $^{36}$Ar.[4] Theoretical calculations of log $ft$ values[5] have since been published which indicated favorable transitions to higher-lying levels in $^{36}$Ar and preliminary results,[6] reported previously, have shown that such transitions did indeed occur.

## II. EXPERIMENT

The decay of $^{36}$K was studied through the $^{36}$Ar$(p,n)^{36}$K$(\beta^+)^{36}$Ar reaction using 18 MeV protons accelerated by the University of Colorado Nuclear Physics Laboratory cyclotron. The bombarding energy was chosen at a peak in the excitation function[1] for optimal yield.

The University of Colorado pneumatic shuttle, or rabbit, system[7] was used to gate the cyclotron beam and to control the transfer of the target between the irradiation position and a shielded counting station 6 m away. Once the target arrived at the low background counting position, the rabbit system could multi-scale an analyzer to obtain sequentially timed spectra. A valved aluminum high-pressure gas rabbit, equipped with 5 $\mu$m Havar entrance and exit windows, was constructed for this experiment to provide a target capable of maintaining up to 7 atm pressure under a moderate beam, yet light enough to keep the shuttle time below 400 msec. For this experiment the target was filled with 99.94% $^{36}$Ar at 4 atm and irradiated for approximately 100 h at 2 $\mu$ a beam current for data runs and for another 45 h for background runs.

The $\gamma$ transitions in $^{36}$Ar following the decay of $^{36}$K were observed with a 34 cm$^3$ closed-end coaxial Ge(Li) detector. High energy $\gamma$ rays were enhanced relative to low energy ones (keeping dead time to acceptable levels) by using a 5 cm lucite $\beta^+$ absorber followed by a 2.4 cm lead attenuator behind the lead collimator. Three classes of spectra were taken for this experiment. For precise measurement of $\gamma$-ray energies and intensities a single 4096-channel spectrum was accumulated for 960 msec following an irradiation of 640 msec. To determine the half-lives of the individual $\gamma$ rays, the output of the Ge(Li) detector was multiscaled into four sequentially timed 1024-channel spectra at 320 msec intervals after 780 msec bombarding periods. Background activity was identified through two different sets of spectra. Half-lives longer than 10 sec were measured through 4096-channel background spectra, accumulated during long beam off periods in the middle and at the end of the 4096-channel data runs. Background half-lives of the same order as $^{36}$K were determined by a separate irradiation of the same target, filled instead with 4 atm of $^4$He, with the same integrated beam current and timing as the multiscaled data run. This allowed an easy visual comparison between the two sets of spectra to determine which peaks resulted from $^{36}$K decay, as well as a quantitative measure of the half-lives associated with the $\gamma$ rays. These spectra will be referred to as the concurrent background spectra and the timed

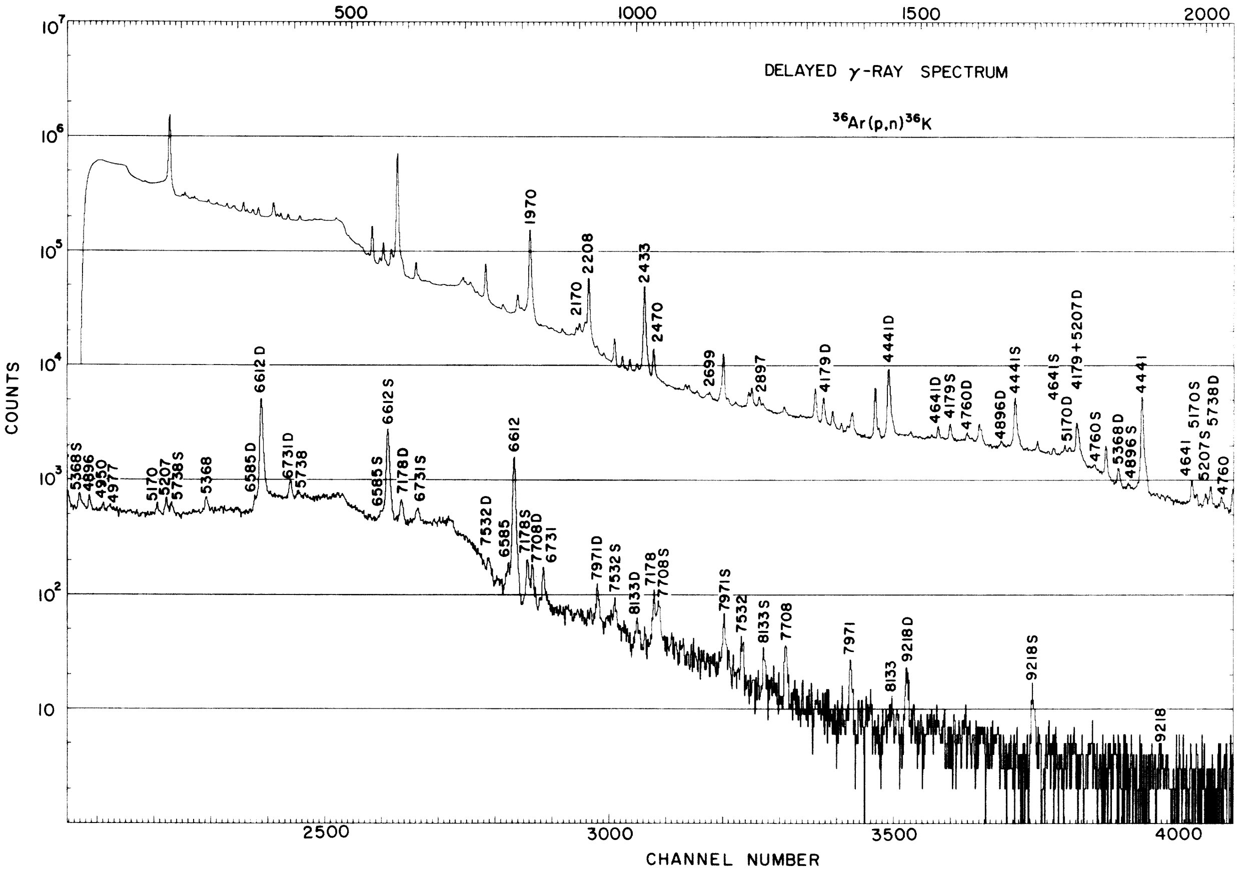


FIG. 1. The spectrum of $\gamma$ rays following the decay of $^{36}K$. Full energy, single escape, and double escape peaks are all labeled. All other peaks are contaminants.

background spectra, respectively.

For all spectra the transit times of the shuttle to and from the counting area were 400–560 msec and 1440 msec, respectively. Variations in the former during a given run could produce intermittent late target arrival at the counting station. To guard against such possible systematic errors, as well as to check on variations in the dead time and drift in the analyzer, spectra were accumulated for two hour periods and saved on magnetic tape, allowing each spectrum to be examined individually, and then summed to construct the final spectra.

### III. ANALYSIS AND RESULTS

Figure 1 shows the 4096-channel delayed $\gamma$-ray spectrum accumulated for the high resolution data runs. All peaks were least squares fitted to obtain areas and peak positions and their errors. Labeled peaks are attributed to the $^{36}K$ decay and their energies and intensities as obtained from these fits are listed in Table I. The $\gamma$-ray energies are error weighted averages over the full-energy, single-escape, and double-escape peaks (FEP, SEP, and DEP, respectively) and have been corrected for recoil. The intensities are similarly averaged and normalized to the 1970 keV $\gamma$ ray. These data are compared with the recoil corrected energies and renormalized intensities of Miller *et al.*[1] The agreement is good.

The decay of these $\gamma$ rays is shown in Fig. 2, with each point representing the summed contributions of the FEP, SEP, and DEP peaks in the sequential 1024-channel spectra. Those $\gamma$ rays which could not be followed due to larger neighboring peaks in the lower (1024) resolution spectra are so indicated in Table I. Since their decay was not determined, their assignment as $^{36}K$ $\beta^+$ delayed $\gamma$'s must be tentative as far as these data are concerned. However, since they are not present in the background runs on the helium target, they are at least due to some reaction on $^{36}Ar$ or a gaseous contaminant, yet do not fit into

TABLE I. Energies and intensities of $\gamma$ rays in $^{36}Ar$ following the decay of $^{36}K$.

| Present experiment | | Ref. 1 | | |
|---|---|---|---|---|
| Energy (keV) | Relative intensity | Energy (keV) | Relative intensity | Transition |
| 9218.35 ± 1.18 | 60 ± 15 | | | g.s. |
| 8132.62 ± 1.40 | 65 ± 20 | | | g.s. |
| 7970.53 ± 0.69 | 155 ± 25 | | | g.s. |
| 7708.24 ± 0.65 | 210 ± 30 | | | g.s. |
| 7531.57 ± 1.04 | 155 ± 30 | | | 9502 → 1970 |
| 7177.62 ± 0.52 | 460 ± 55 | | | g.s. |
| 6730.53 ± 0.50 | 550 ± 70 | | | g.s. |
| 6612.13 ± 0.37 | 8140 ± 590 | 6613.4 ± 0.8 | 9250 ± 1150 | g.s. |
| 6585.05 ± 0.49 [a] | 195 ± 65 | | | 8556 → 1970 |
| 5738.24 ± 0.55 | 440 ± 70 | | | 7708 → 1970 |
| 5367.52 ± 0.47 | 665 ± 80 | | | 7338 → 1970 |
| 5206.53 ± 0.42 | 385 ± 90 | | | 7177 → 1970 |
| 5169.51 ± 0.77 | 370 ± 75 | | | 7140 → 1970 |
| 4977.15 ± 1.05 [a] | 170 ± 60 | | | g.s. |
| 4950.04 ± 0.91 [a] | 195 ± 60 | | | g.s. |
| 4896.27 ± 1.09 | 420 ± 75 | | | 6867 → 1970 |
| 4759.60 ± 0.72 | 545 ± 85 | | | 6731 → 1970 |
| 4640.96 ± 0.50 | 875 ± 95 | 4644.0 ± 1.4 | <1100 | 6612 → 1970 |
| 4440.79 ± 0.34 | 9750 ± 600 | 4442.0 ± 0.6 | 11 800 ± 650 | g.s. |
| 4178.53 ± 0.41 | 2500 ± 100 | 4180.7 ± 1.0 | 3900 ± 890 | g.s. |
| 2896.97 ± 0.34 [a] | 1210 ± 85 | | | 7338 → 4441 |
| 2699.28 ± 0.45 [a] | 470 ± 35 | | | 7140 → 4441 |
| 2470.46 ± 0.42 | 5830 ± 230 | 2472.1 ± 0.8 | 5570 ± 890 | 4441 → 1970 |
| 2433.43 ± 0.21 | 38 800 ± 1750 | 2433.8 ± 0.4 | 41 800 ± 5100 | 6612 → 4179 |
| 2207.83 ± 0.30 | 36 500 ± 1670 | 2208.4 ± 0.4 | 36 700 ± 5100 | 4179 → 1970 |
| 2170.29 ± 0.20 [a] | 3700 ± 400 | 2171.6 ± 0.9 | 2800 ± 630 | 6612 → 4441 |
| 1970.44 ± 0.46 | 100 000 ± 10 300 | 1969.9 ± 0.5 | 100 000 ± 10 100 | g.s. |

[a] Decay of $\gamma$ ray not followed.

known decay schemes for such nuclei. Furthermore, they can be placed in the $^{36}K$ decay scheme with good agreement with known levels and branching ratios.

Since the $\gamma$-ray energy values in Table I have already been recoil corrected, they can be combined to find the best fit for $\gamma$ rays summing to a given level. These values are shown in Table II as the excitation energies determined by this experiment. Comparison with those determined by Refs. 3 and 4 is also shown. The branching ratios for each of these levels are listed in Table III, where each entry is a triad; the uppermost giving the value cited in Ref. 4; the middle, the value cited in Ref. 3; and the present experiment, the lowest. The branching ratios have been determined for this experiment allowing for other possible branches which may have been obscured by contaminants or overlying $^{36}K$ peaks. If a branch was previously reported in Refs. 3 and 4 but would have been obscured by interfering peaks, the branching ratios of Ref. 3 were adopted, and in such cases the ratios are obviously not separate determinations. In all cases of unseen branches, the missing $\gamma$-ray energies fell in portions of the spectra where they should *not* have been seen; i.e., none of the $\gamma$ rays attributed to $^{36}K$ decay were in conflict with the known branching ratios for the specified levels. The unseen strength for these levels was used as indicated in Table III to deduce $\beta^+$ intensities and the log $ft$ values. The final decay scheme so constructed, together with log $ft$ values, is shown in Fig. 3.

Figure 4 compares the timed background spectrum taken with $^4He$ and the data spectra by summing all four 1024-channel spectra. Since the spectra were taken for the same total integrated beam current, and dead times were approximately the same, this affords a good comparison of the contributions from reactions on the target body and windows. Air contaminants were present in both spectra, although to a much smaller degree in the $^{36}K$ spectrum. Analysis of the timed background spectra, their decay, and the concurrent background spectra shows that 20 nuclides are produced from the Havar foil windows and their brass mounts. There are also two $\gamma$ rays produced from competing reactions on $^{36}Ar$, residual activity in the concrete walls of the counting station, and $^{14}O$ and $^{16}N$ $\gamma$ rays from air contam-

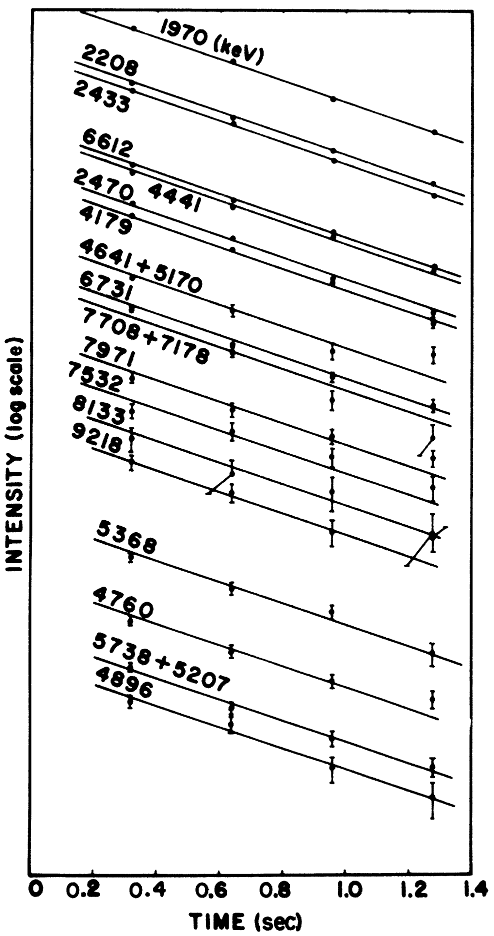


FIG. 2. The decay of $\gamma$ rays associated with transitions in $^{36}Ar$.

inants. Assignment of $\gamma$ rays to specific nuclides was made on the basis of both energy and intensity of known branches in their decays. The total area under all peaks was consistently accounted for in all spectra with few exceptions, with most of those occurring in the low energy region of the spectra where it was impossible to obtain good decay statistics because of the large number of competing peaks. For this reason, there are no low energy (less than 1970 keV) data quoted here for $^{36}Ar$ transitions, which is also the region of most unseen branches. On the basis of all available information, background contributions were subtracted unambiguously from all $^{36}Ar$ peaks.

Although contaminant peaks were a hindrance in extracting $^{36}Ar$ peak areas, they provided copious data points for both the energy and efficiency calibrations. Prominent $\gamma$ rays from the decay of $^{66}Ga$, $^{64}Ga$, $^{60}Cu$, $^{56}Co$, $^{57}Ni$, $^{92}Tc$, $^{55}Co$, $^{63}Zn$, $^{94}Tc$, and $^{52}Mn$ provided energy calibration points from 670 to 4807 keV. At higher energies a pulser was used to determine the near linear behavior of the analyzer. The final energy calibration demanded the best fit to the contaminant peaks, to the pulser, and to the proper spacing between prominent FEP, SEP, and DEP peaks.

The efficiency calibration used a smooth fit to the $\gamma$-ray intensities from the $^{56}Co$ decay[8] to establish the low energy portion (487 to 3550 keV) of the FEP curve. Proton capture resonances at 1417 and 1318 keV in the $^{23}Na(p, \gamma)$ reaction provided data on the 13 052 → 4123 → 1369 keV and 12 957 → 1369 → 0 keV cascades, respectively. Values obtained from the smoothed efficiency curve at 2754 and 1369 keV then provided relative efficiencies at 8929 and 11588 keV, respectively, from the known branching ratios.[9] The peak areas ratios DEP/FEP, SEP/FEP, and DEP/SEP were determined from intense transitions in the decays of $^{66}Ga$, $^{64}Ga$, $^{60}Cu$, $^{56}Co$, $^{57}Ni$, and $^{36}K$ and from the capture resonance data, and fitted to smooth curves to obtain the DEP and SEP curves. A final check on the shapes of all efficiency curves was made by converting published data on coaxial Ge(Li) detectors[10] to our different shielding, and extrapolating to a 34 $cm^3$ detector. The agreement was remarkably good, falling within 5% of all the smoothed curves.

The half-life of $^{36}K$ was determined from the weighted average of values found from least squares fits to the decay of individual peak areas in the four multiscaled 1024-channel spectra, after appropriate dead-time corrections. A second determination was made by subtracting the summed timed background spectra from the

TABLE II. Excitation energies of levels in $^{36}Ar$ seen in $^{36}K$ decay.

| Present experiment | Ref. 3 | Ref. 4 |
|---|---|---|
| 1970.4 ± 0.5 | 1970.39 ± 0.05 | 1970.2 ± 0.3 |
| 4178.5 ± 0.5 | 4178.33 ± 0.11 | 4178.1 ± 0.7 |
| 4440.8 ± 0.5 | 4440.1 ± 0.2 | 4440.2 ± 0.5 |
| 4950.0 ± 0.9 | 4951.9 ± 0.5 | 4950.9 ± 0.5 |
| 4977.2 ± 1.1 | 4974.05 ± 0.19 | 4974.1 ± 0.7 |
| 6611.8 ± 0.5 | 6610.8 ± 0.3 | 6611.4 ± 0.5 |
| 6730.5 ± 0.7 | 6729 ± 9.0 | 6724 ± 2 |
| 6866.7 ± 1.1 | 6868.5 ± 1.0 | 6865.2 ± 1 |
| 7140.1 ± 0.9 | 7139.5 ± 0.4 | 7140.5 ± 1 |
| 7177.4 ± 0.6 | 7178.7 ± 0.9 | 7179.0 ± 0.5 |
| 7337.9 ± 0.7 | 7335.6 ± 0.7 | 7338.5 ± 1 |
| 7708.4 ± 0.8 | 7710.7 ± 1.8 | 7711.1 ± 1.5 |
| 7970.5 ± 0.7 | 7972 ± 10 | ··· |
| 8132.6 ± 1.4 | 8136 ± 10 | 8132 ± 2 |
| 8555.5 ± 0.6 | 8550 ± 30 | ··· |
| 9218.4 ± 1.2 | 9220 | 9220 |
| 9502.0 ± 1.1 | 9501 | 9502 |

TABLE III. Branching ratios of $^{36}$Ar levels seen in $^{36}$K decay. Entries are in the order: Ref. 4, Ref. 3, present experiment.

| $E_x$ (keV) | $J^\pi$ | 0 $0^+$ | 1970 $2^+$ | 4179 $3^-$ | 4441 $2^+$ | Others $E_x$ (%) |
|---|---|---|---|---|---|---|
| 1970 | $2^+$ | 100 | | | | |
| | | 100 | | | | |
| | | 100 | | | | |
| 4179 | $3^-$ | 7.7 ± 0.6 | 92.3 ± 0.6 | | | |
| | | 5.9 ± 0.6 | 94.1 ± 0.6 | | | |
| | | 6.0 ± 0.6 | 94.0 ± 0.6 | | | |
| 4441 | $2^+$ | 64 ± 2 | 36 ± 2 | | | |
| | | 65 ± 3 | 35 ± 3 | | | |
| | | 62.5 ± 2.5 | 37.5 ± 2.5 | | | |
| 4950 | $2^{+}$ [a] | 84 ± 5 | 16 ± 5 | <2 | ··· | ··· |
| | | 86 ± 4 | 14 ± 4 | <2 | ··· | ··· |
| | | 84 | ··· | ··· | ··· | Unknown 16 |
| 4977 | $2^-$ | 19 ± 2 | 5 ± 2 | 76 ± 2 | <0.3 | ··· |
| | | 16 ± 2 | 4.0 ± 0.9 | 80 ± 3 | ··· | ··· |
| | | 19 | ··· | ··· | ··· | Unknown 81 |
| 6612 | $2^+, T=1$ | 22 ± 3 | <5 | 78 ± 3 | ··· | ··· |
| | | 15 ± 3 | <7 | 85 ± 3 | <6 | ··· |
| | | 15.8 ± 1.7 | 1.7 ± 0.3 | 75.3 ± 2.5 | 7.2 ± 1.1 | ··· |
| 6731 | $(1, 2)^+$ | 70 ± 10 | ··· | ··· | ··· | Unknown 30 |
| | | ··· | ··· | ··· | ··· | ··· |
| | | 48 ± 7 | 52 ± 7 | ··· | ··· | ··· |
| 6867 | | 25 ± 5 | 75 ± 5 | ··· | ··· | ··· |
| | | 51 ± 12 | 49 ± 12 | ··· | ··· | ··· |
| | | <23 | 77 | ··· | ··· | ··· |
| 7140 | $3^+$ | <2 | 48 ± 5 | <3 | 52 ± 5 | ··· |
| | | ··· | 44 ± 7 | ··· | 56 ± 7 | ··· |
| | | ··· | 44 ± 7 | ··· | 56 ± 7 | ··· |
| 7177 | $(1, 2)^+$ | 70 ± 10 | 30 ± 10 | ··· | ··· | ··· |
| | | 63 ± 13 | 37 ± 13 | ··· | ··· | ··· |
| | | 50 ± 7 | 50 ± 7 | ··· | ··· | ··· |
| 7338 | $3^{+}$ [a], $T=1$ | <3 | 26 ± 3 | 9 ± 2 | 54 ± 2 | 4415(11 ± 2) |
| | | <6 | 31 ± 5 | 17 ± 4 | 52 ± 5 | ··· |
| | | ··· | 29 ± 4 | ··· | 51 ± 4 | Unknown 20 |
| 7708 | $(1-3)^-$ | 35 ± 10 | 65 ± 10 | ··· | ··· | ··· |
| | | 39 ± 7 | ··· | ··· | ··· | Unknown 61 ± 7 |
| | | 32 ± 8 | 68 ± 8 | ··· | ··· | ··· |
| 7971 | $(1, 2)^+$ | ··· | ··· | ··· | ··· | ··· |
| | | ··· | ··· | ··· | ··· | ··· |
| | | 100 | ··· | ··· | ··· | ··· |
| 8133 | | 60 ± 7 | 40 ± 7 | ··· | ··· | ··· |
| | | ··· | ··· | ··· | ··· | ··· |
| | | 60 | ··· | ··· | ··· | Unknown 40 |
| 8556 | $2^+, T=1$ | ··· | ··· | ··· | ··· | ··· |
| | | ··· | ··· | ··· | ··· | ··· |
| | | ··· | 100 | ··· | ··· | ··· |
| 9218 | $1^{(+)}, T=1$ | 34 | 50 | <1 | 11 | 4328(0.4), 4950(0.8), 4977(3), 5836(0.8) |
| | | ··· | ··· | ··· | ··· | ··· |
| | | 34 | ··· | ··· | ··· | Unknown 66 |
| 9502 | 2, 3, 4 [a] | 1 | 57 | <1 | 14 | 4415(4), 6612(16), 7338(8) |
| | | ··· | ··· | ··· | ··· | ··· |
| | | ··· | 57 | ··· | ··· | Unknown 43 |

[a] All assignments are from Ref. 3 unless indicated to show Ref. 4.

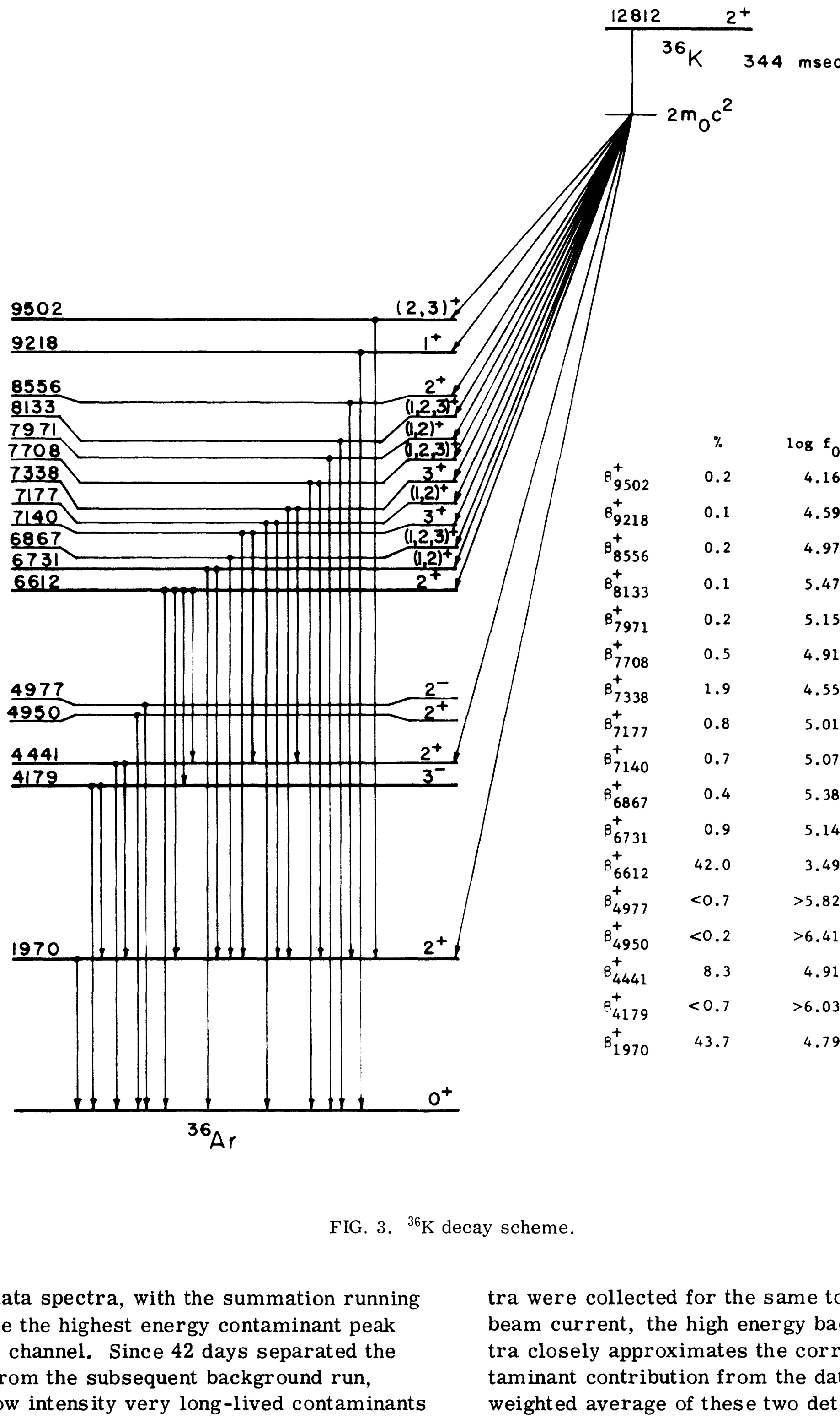


| | % | log $f_0t$ |
|---|---|---|
| $\beta^+_{9502}$ | 0.2 | 4.16 |
| $\beta^+_{9218}$ | 0.1 | 4.59 |
| $\beta^+_{8556}$ | 0.2 | 4.97 |
| $\beta^+_{8133}$ | 0.1 | 5.47 |
| $\beta^+_{7971}$ | 0.2 | 5.15 |
| $\beta^+_{7708}$ | 0.5 | 4.91 |
| $\beta^+_{7338}$ | 1.9 | 4.55 |
| $\beta^+_{7177}$ | 0.8 | 5.01 |
| $\beta^+_{7140}$ | 0.7 | 5.07 |
| $\beta^+_{6867}$ | 0.4 | 5.38 |
| $\beta^+_{6731}$ | 0.9 | 5.14 |
| $\beta^+_{6612}$ | 42.0 | 3.49 |
| $\beta^+_{4977}$ | <0.7 | >5.82 |
| $\beta^+_{4950}$ | <0.2 | >6.41 |
| $\beta^+_{4441}$ | 8.3 | 4.91 |
| $\beta^+_{4179}$ | <0.7 | >6.03 |
| $\beta^+_{1970}$ | 43.7 | 4.79 |

FIG. 3. $^{36}K$ decay scheme.

summed data spectra, with the summation running from above the highest energy contaminant peak to the last channel. Since 42 days separated the data run from the subsequent background run, only the low intensity very long-lived contaminants remained in the target. The high energy portion of the background spectra is then primarily due to the activity produced during the background run itself. Because both the data and background spectra were collected for the same total integrated beam current, the high energy background spectra closely approximates the corresponding contaminant contribution from the data run. The weighted average of these two determinations yields a half-life of $344 \pm 3$ msec, with most of the error due to systematic errors. The comparison with previous experiments[1,2,11-13] is shown in Table IV.

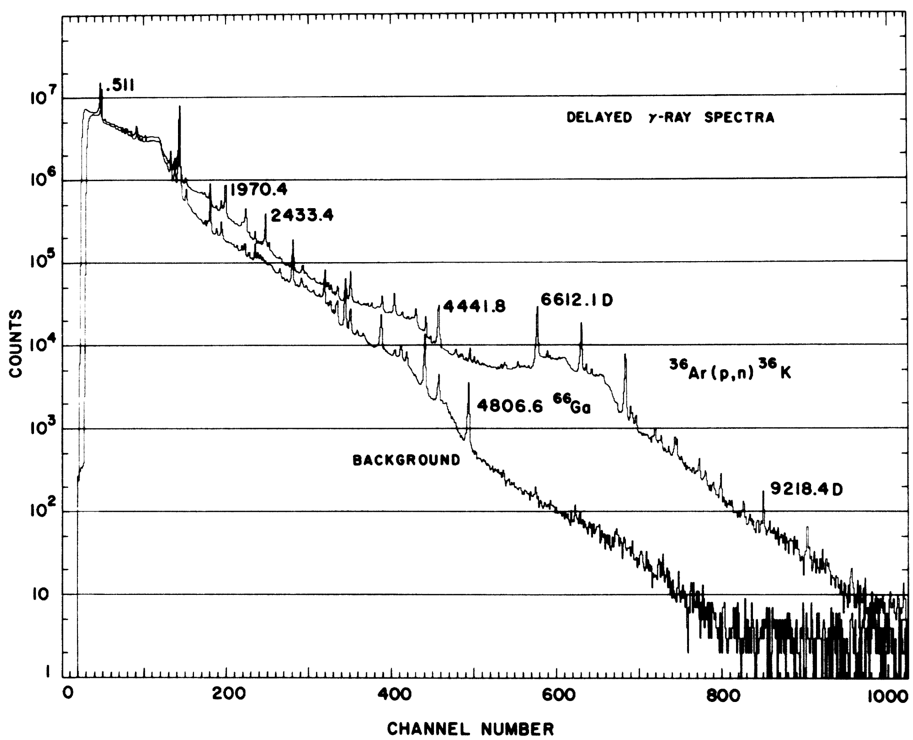


FIG. 4. Comparison of spectra obtained using a 4 atm gas rabbit filled with 99.94% $^{36}$Ar and with $^{4}$He. There is a slight difference in the energy calibrations of the two spectra.

## IV. CONCLUSIONS

The log $ft$ values cited for $\beta^+$ transitions shown in Fig. 3 are taken from tabulated log $f_0t$ values,[14] and all fall into the range of values for allowed transitions.[15] The spins and parities of these levels are then restricted to $1^+$, $2^+$, or $3^+$. However, the experimental evidence implying the existence of the $\beta^+$ branches varies considerably, and individual levels will be discussed on the basis of that evidence.

### A. 7708, 7177, 6731, 6612, and 4441 keV levels

These level assignments have been corroborated by at least two transitions whose decay has been measured. In all cases the agreement with previous experiments is good (see Tables I–III) except for the parity of the 7708 keV level, for which we assign a positive value.

TABLE IV. Comparison of $^{36}$K half-life measurements.

| Half-life (msec) | Ref. |
|---|---|
| 265 ± 25 | 2 |
| 345 ± 5 | 11 |
| 336 ± 4 | 12 |
| 342 ± 28 | 13 |
| 341 ± 6 | 1 |
| 344 ± 3 | Present experiment |

### B. 7738 and 7140 keV levels

Both levels are associated with two $\gamma$ rays seen in the experiment, just one of which was strong enough to have a measurable decay in this experiment. Agreement with previous experiments is again good.

### C. 9502, 9218, 8133, 7971, 6867, and 1970 keV levels

Assignments to these levels have been made on the basis of just one $\gamma$ ray whose decay was followed. In all cases the transition energy is in good agreement with known energy levels, there are no conflicts with known spins and parities, and any previously determined branching ratios predict $\gamma$ rays which in this experiment are masked by contaminant peaks. As above, branches from higher levels cannot account for the observed intensity, and all contributions predicted from known branching ratios from higher levels have been accounted for in the $\beta^+$ intensities shown. Assignment of the $\gamma$ rays to transitions between other levels based on energy summation would lead to conflicts; e.g., the 7971 keV $\gamma$ ray as a 9941–1970 transition would yield a prohibitively small log *ft*.

### D. 8556 keV level

Since only one $\gamma$ ray is observed for this transition, and its decay was not measured, this assignment is quite tentative. The existence of the branch is then postulated solely on the basis of the disappearance of the $\gamma$ ray in the background spectra and its failure to fit into the decay schemes of possible competing reactions. Assignment of the $\gamma$-ray transition to other levels would result in conflicts and the intensity is not attributable to cascades from higher levels.

### E. 4179 keV level

Although two transitions were seen for this level, and their decays measured, no definite assignment could be made for this level since the $\beta^+$ intensity would be implied from the subtraction of two larger numbers representing the observed $\gamma$ transitions and $\gamma$ transitions feeding the 4179 keV level from higher lying states. The upper limit given leads to a log *ft* commensurate with a first-forbidden $\beta^+$ transition, which would be predicted to this $3^-$ level.

### F. 4977 and 4950 keV levels

The evidence supporting these branches is the same as for the 8556 keV level except that here errors in the branching ratios of higher lying levels lead to an uncertainty in the intensity feeding these levels which is nearly as great as the transitions themselves. An upper limit on the intensities is then all that may be determined.

$\beta^+$ branches for the decay of $^{36}$K may therefore be assigned to 13 levels in $^{36}$Ar, together with one tentative assignment for the 8556 keV level. Of these 13 branches, 5 are presented in the shell-model calculations of Ref. 5, with two branches predicted to $T=1$ levels in $^{36}$Ar at 8.68 ($1^+$) and 8.36 ($3^+$) MeV. The predicted log *ft*'s for these transitions are 4.85 and 4.23, respectively. This is in remarkably good agreement with the experimentally determined log *ft* values of 4.59 and 4.55 for branches to the $T=1$ levels at 9218 ($1^+$) and 7338 ($3^+$) keV.

### ACKNOWLEDGMENTS

It is a pleasure to acknowledge the participation of Paul Ingalls in experiments to determine the efficiency of the Ge(Li) detector. The author is particularly indebted to him, Clyde Zaidins, and Roger Bunting for their encouragement and invaluable discussions. The help of Owen Sharp in the data reduction and preparation of figures is gratefully acknowledged.

---

†Work supported in part by the U. S. Energy Research and Development Administration.

*Present address: Science Applications, Incorporated, McLean, Virginia 22101.

[1]D. W. Miller *et al.*, Phys. Rev. C 6, 869 (1972).

[2]R. E. Berg, J. L. Snelgrove, and E. Kashy, Phys. Rev. 153, 1165 (1967).

[3]P. M. Endt and C. Van Der Leun, Nucl. Phys. A214, 1 (1973). $Q_{\beta^+} = 12\,812 \pm 8$ keV is quoted for the $^{36}$K decay. This $Q$ value is cited as $12\,810 \pm 8$ keV in the 1974 revision of the Wapstra-Gove Mass Tables (private communication).

[4]P. M. Johnson, M. A. Meyer, and D. Reitmann, Nucl. Phys. A218, 333 (1974).

[5]W. A. Lanford and B. H. Wildenthal, Phys. Rev. C 7, 668 (1973).

[6]M. J. Fritts, Bull. Am. Phys. Soc. 18, 1399 (1973).

[7]M. J. Fritts and C. S. Zaidins, FRIT-ZAID series on nuclear instrumentation, University of Colorado Internal Report, 1974 (unpublished).

[8]D. C. Camp and G. L. Meredith, Nucl. Phys. A166, 349 (1971).

[9]B. P. Singh and H. C. Evans, Nucl. Instrum. Methods 97, 475 (1971).

[10]H. Seyfarth, A. M. Hassan, B. Hrastnik, P. Göttel, and W. Delang, Nucl. Instrum. Methods 105, 301 (1972).

[11]A. A. Jaffe *et al.*, Phys. Rev. C 3, 2489 (1971).

[12]D. R. Goosman, K. W. Jones, E. K. Warburton, and D. E. Alburger, Phys. Rev. C 4, 1800 (1971).

[13]C. E. Moss, C. Détraz, C. S. Zaidins, and D. J. Frantsvog, Phys. Rev. C 5, 1122 (1972).

[14]N. B. Gove and M. J. Martin, Nucl. Data B10, 205 (1971).

[15]S. Raman and N. B. Gove, Phys. Rev. C 7, 1995 (1973).